Eur. Phys. J. D **30**, 15–22 (2004)
DOI: 10.1140/epjd/e2004-00071-9

THE EUROPEAN PHYSICAL JOURNAL D

Investigation of highly excited states of calcium by three-photon ionization

R.S. Dygdała[1], A. Zawadzka[2], D. Lisak[2,a], P. Płóciennik[2], and R.S. Trawiński[2]

[1] Instytut Matematyki, Akademia Bydgoska im. Kazimierza Wielkiego, Chodkiewicza 30, 85-064 Bydgoszcz, Poland
[2] Instytut Fizyki, Uniwersytet Mikołaja Kopernika w Toruniu, ul. Grudziądzka 5/7, 87-100 Toruń, Poland

Received 9 April 2003 / Received in final form 29 September 2003
Published online 18 May 2004 –

Abstract. The three-photon ionization in Ca from $4s^2\ ^1S_0$ ground state is studied. The two-photon process is a near — resonance process with one of the following bound states: $4s4d\ ^1D_2$, $4p^2\ ^3P_2$, $4s6s\ ^1S_0$, $4p^2\ ^1D_2$ and $4p^2\ ^1S_0$ while the third photon reach either directly the continuum or one of the autoionizing states. The succession of bound states as well as the transitions above the ionization limit are discussed. The dynamics of the multiphoton excitation processes is also discussed and radiative decay of $4p^2\ ^1S_0$ Ca state with two-photon excitation as well as (the measured) decay times of the Ca autoionizing states using the proper line profiles for different quantum numbers has been determined.

PACS. 32.70.-n Intensities and shapes of atomic spectral lines – 32.70.Cs Oscillator strengths, lifetimes, transition moments – 32.80.Fb Photoionization of atoms and ions – 32.80.Rm Multiphoton ionization and excitation to highly excited states (e.g., Rydberg states)

1 Introduction

A progress in the physics of lasers, masers and synchrotron radiation has stimulated numerous new developments in both experimental and theoretical investigations of the interaction of radiation with atomic systems. As a result of such an interaction atoms may be excited or ionized. The latter process may in particular occur through an excitation and a decay of autoionizing states. The measured lifetimes of these states as well as lifetimes of atomic and molecular Rydberg states disagree often by several orders of magnitude from those expected theoretically. The reason, of such discrepancies have already been discussed [1–3] and is still interesting [4]. For instance, the line profiles of multiphoton optical transitions to the Rydberg states depend not only on the radiative decays of those states but also, on several nonradiative decay channels such as those through autoionizing state. In such a case the analysis of decay processes of autoionizing states is important.

The studies of the lowest autoionizing states of alkaline earths can be performed by using only one or two laser beams and have been performed earlier [5–10]. The resonances to autoionizing states of Ca which are located in the higher part of continuum can be reached by the three-photon transition [11–14]. In calcium as in other elements possessing two ns valence electrons, the electron correlations in the valence shell are sufficiently strong to allow for a reasonable probability of exciting both valence electrons simultaneously. An ionization in Ca can thus occurs either via a transfer of a single electron directly to the continuum or via a transfer of one electron to the continuum accompanied by an excitation of the other electron or via a simultaneous excitation of both electrons, one of them being transferred to an autoionization state which later decays. An important question is which of these mechanism dominates.

In the present study two-photon resonant processes due to the bound Ca states as well as three-photon resonances due to autoionizing Ca states are engaged. The three-photon ionization in Ca is performed by two-photon transitions from the $4s^2\ ^1S_0$ ground state to the vicinity of excited states: $4s4d\ ^1D_2$, $4p^2\ ^3P_2$, $4s6s\ ^1S_0$, $4p^2\ ^1D_2$ and $4p^2\ ^1S_0$, where the third photon ionizes the atom. Simultaneously three-photon ionization through the autoionizing states has been observed. An excimer — dye-laser, 10 ns duration, exciting the atomic system with the laser intensity of 10^8 W/cm^2 was used. A mass spectrometer was employed in order to resolve the Ca^+ ions and to improve the signal to noise ratio. All the observed resonances are manifested as an increase in the ion number. Additionally the radiation decay of two-photon excited $4p^2\ ^1S_0$ state, for laser intensities of 10^4 W/cm^2 have been measured. The range of the wavenumber under investigation, 18 600 cm^{-1} to 20 930 cm^{-1} for one photon of laser excitation, has been explored. All measurements have been performed for such laser intensities and Ca beam densities that collective effects and charge effects [13,15–19] do not modify the multiphoton ionization.

[a] e-mail: dlisak@phys.uni.torun.pl

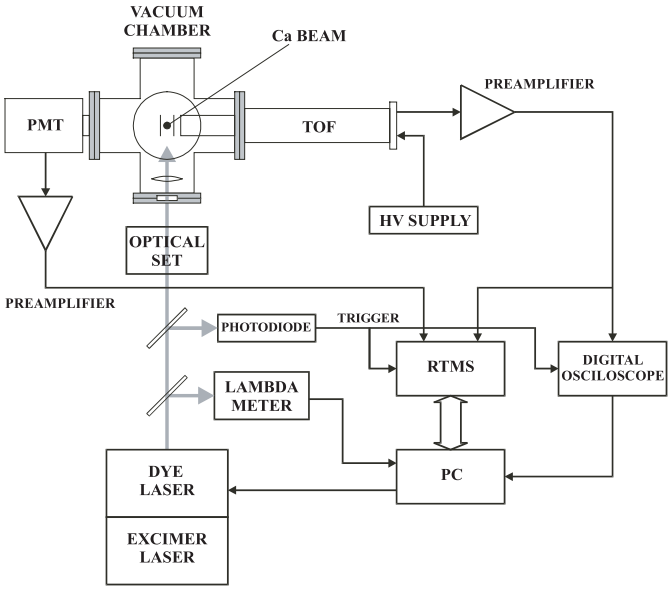

Fig. 1. The experimental set-up. TOF – time-of-flight mass spectrometer, RTMS – real time multichannel scaler, PMT – photomultilier tube. Optical set include linear and circular polarizers. For some measurements the digital LeCroy oscilloscope was used instead of the RTMS (see text for the detailed description).

The selection rules and the transition sequences during multiphoton excitation depend on the laser polarization. The analysis of Ca photoionization spectrum in the examined range of wavenumbers has revealed the positions of the bound states excited by two-photons: $4s6s\ ^1S_0$, $4p^2\ ^1D_2$ and $4p^2\ ^1S_0$. The comparison of the shapes of the signal due to the autoionizing transitions have been performed within the Fano model [20]. The role of two possible channels (autoionization with or without resonant intermediate states and direct) of the multiphoton ionization has been considered. The analysis of the Fano autoionizing line profiles using the computer procedure allowed us to determine the measured decays of autoionizing states for both, low and high quantum numbers of measured transitions series.

The main goal of this paper is the investigation of a dynamic of processes in Ca atoms due to the multiphoton ionization. One has to stress that the method used is based on a direct observations of the ionization product combined with a multiphoton excitation. A high sensibility of such a method allowed for an observation of the autoionizing states close to the limit of the series and measurements of their Fano autoionizing shapes. Due to the multiphoton, two-photon resonant character of the excitation one could analyze the transitions to the final states with both $J = 1$ and $J = 3$.

2 Experiment

The experimental apparatus is shown in Figure 1 and has been described in detailes in our earlier papers [13,19]. An oven — a source of Ca beam and a time-of-flight (TOF) spectrometer are placed in the vacuum chamber. The pressure in the vacuum chamber associated with operating Ca oven is of order of 10^{-7} mbar.

The Ca effusive atomic beam produced by the oven had a diameter 0.4 cm in the interaction region where the laser beam and Ca atomic beam intersect and where ions and electrons are created. The density of the Ca beam is in range of $10^{11}-10^{12}$ atoms/cm^3 [21]. The excitation system is based on excimer laser pumped (308 nm) dye laser delivering tunable radiation with 0.5 cm^{-1} bandwidth and 10 ns pulse duration. The polarization of the excitation laser beam was linear (polarizing prism plus $\lambda/2$ Fresnel rhomb) or circular (polarizing prism plus $\lambda/4$ Fresnel rhomb) in all of our measurements and focused in the Ca effusive beam. In both cases polarization of laser beam was greater than 99%.

The method of ions detection is based on an single ion counting or an integrated ion signal measuring. The COMSTOCK, model TOF 101 mass spectrometer with the tandem multichannel plate detector [12,13,19] allowed us to resolve the Ca^+ ions only. The ion signal from the multichannel plate detector have been measured using a real time multichannel scaler or a LeCroy 9370, 1 GHz digital oscilloscope [22]. The procedure of measurements described above gives us the time of flight distribution of the detected Ca^+ ions [13,19]. Those measurements were performed for laser intensities in the range of 10^8 W/cm^2.

The method of the Ca bound states lifetime measurements using the 10 ns pulse dye laser depend on registration of the Ca fluorescence signal in a real time. The Hamamatsu R943-02 photomultiplier with the 2 ns rise time of pulses have been used in the single photon counting mode. The Ca fluorescence signal passes through an interference filter and reaches the photomultiplier. The photon signal from the photomultiplier detector was composed of a train of pulses amplified [23] and fed to an input of a real time multichannel scaler [22]. The procedure of the bound Ca states lifetime measurements described above was performed for different laser intensities in the range of 10^4 W/cm^2 and has been averaged over 10^4 laser shots. It gives us the lifetime of the bound state for a selected laser power.

3 Two-photon bound state transitions

Calcium atoms in the thermal atomic beam are excited from the $4s^2\ ^1S_0$ ground state to the region of the $4s4d\ ^1D_2$, $4p^2\ ^3P_2$, $4s6s\ ^1S_0$, $4p^2\ ^1D_2$ and $4p^2\ ^1S_0$ states by two photons from a pulsed dye laser (Fig. 2). The atoms can be photoionized by a third photon from the same laser and overcome the ionization limit of Ca (49 306 cm^{-1}) [24,25]. Moreover, in the examined wavenumber $\nu = 3\nu_L$ (where ν_L is the laser photon wavenumber) region the manifold of autoionizing states was found and identified [11,13,14,25]. We have to notice that in our earlier papers [12,13,19] the succession of $4s6s\ ^1S_0$ and $4p^2\ ^1S_0$ have been taken according to the paper by Moore [24].

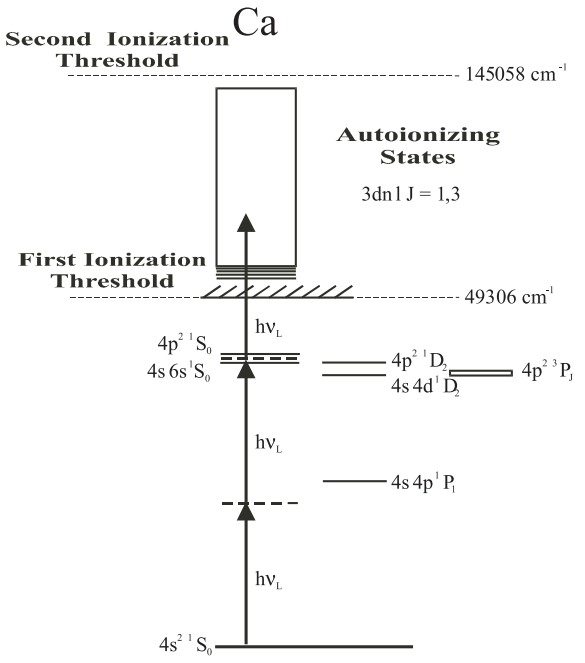

Fig. 2. A simplified energy diagram of Ca. The laser frequency corresponds to the two-photon resonance from the $4s^2\ {}^1\mathrm{S}_0$ ground state to one of excited states: $4s6s\ {}^1\mathrm{S}_0$, $4s4d\ {}^1\mathrm{D}_2$, $4p^2\ {}^1\mathrm{S}_0$, $4p^2\ {}^1\mathrm{D}_2$, $4p^2\ {}^3\mathrm{P}_2$.

3.1 The selection rules

The atom/ion–radiation field interaction can be characterized by selection rules concerning the change of the quantum numbers representing those atoms or ions. The selection rules [26] and the transition sequences during multiphoton excitation depend on the laser polarization. For linear polarization $\Delta M = 0$ and for circular polarization $\Delta M = \pm 1$. Taking into account that the L-S coupling is not a good approximation in calcium we have to expect that the simple selection rules brake down and only the selection rule for J should work [11]. In our paper we use the L-S coupling notation for simplicity.

In our measurements we used the linear and circular polarization of the laser beam. In Figures 3 and 4 the ion signal is presented as a function of the wavenumber for the aprriopriate transitions from the ground Ca state. From Figure 3 ($4s^2\ {}^1\mathrm{S}_0$ to $4s6s\ {}^1\mathrm{S}_0$ and $4p^2\ {}^1\mathrm{D}_2$) it is seen that the height of the maximum of the ion signal for two-photon resonant three-photon ionization ($4s^2\ {}^1\mathrm{S}_0$–$4p^2\ {}^1\mathrm{D}_2$) does not depend on the laser beam polarization what agree with the theoretical predictions. Two-photon transition to the state $4p^2\ {}^1\mathrm{D}_2$ ($J = 2$ and $M = 0, \pm 1, \pm 2$) is allowed according to the selection rules depending on laser beam polarization because the ground state of Ca is characterized by $J = 0$ and $M = 0$ and we can take into account that the intermediate state reached by the first photon is $4s4p\ {}^1\mathrm{P}_1$ state ($J = 1$ and $M = 0, \pm 1$). For other schemes of two-photon resonance three-photon ionization ($4s^2\ {}^1\mathrm{S}_0$–$4s6s\ {}^1\mathrm{S}_0$, Fig. 3; $4s^2\ {}^1\mathrm{S}_0$–$4p^2\ {}^1\mathrm{S}_0$, Fig. 4), the ion signals are different for different polarization of the laser beam. In this case the intermediate state reached by the first photon is also $4s4p\ {}^1\mathrm{P}_1$ state. For the two-photon resonance both states $4s6s\ {}^1\mathrm{S}_0$ and $4p^2\ {}^1\mathrm{S}_0$ are characterized by the quantum numbers $J = 0$ and $M = 0$. In this case such transitions are allowed for linear polarization while are forbidden for circular polarization.

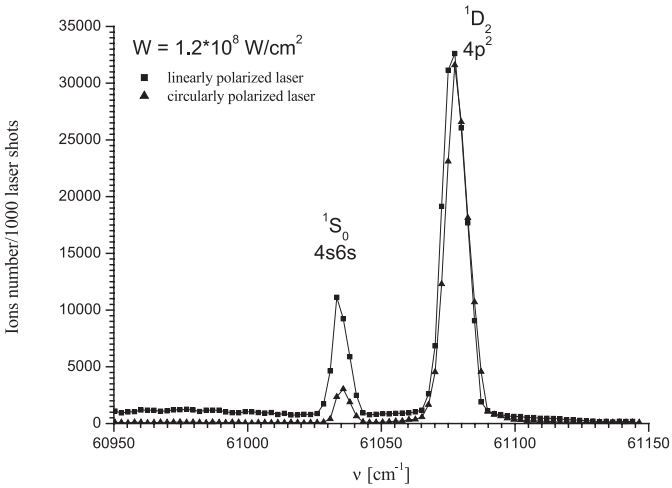

Fig. 3. Ionization yield for two-photon resonant through $4s6s\ {}^1\mathrm{S}_0$ and $4p^2\ {}^1\mathrm{D}_2$ states, three-photon ionization as a function of wavenumbers $\nu = 3\nu_L$ for linear and circular laser beam polarization.

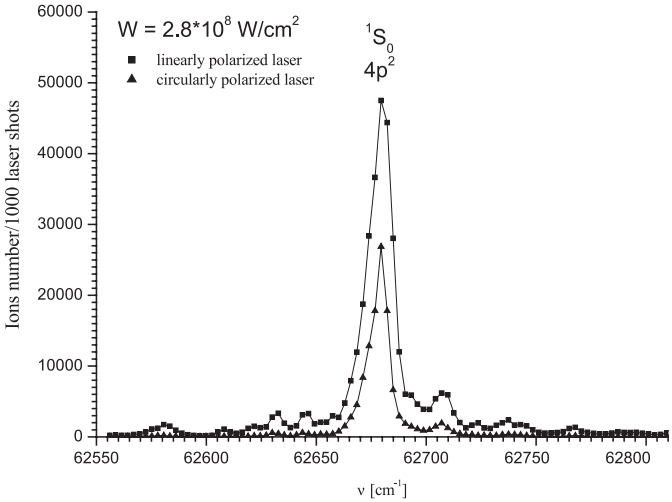

Fig. 4. Ionization yield for two-photon resonant through $4p^2\ {}^1\mathrm{S}_0$ state, three-photon ionization as a function of wavenumbers $\nu = 3\nu_L$ for linear and circular laser beam polarization.

The observation of nonzero ion signals in the situation in which two-photon resonances are forbidden can be explained by a possibility of other intermediate states introduced in the excitation process. For such a heavy atom as Ca we should take into account [11] of spin-orbit coupling. The rule of $\Delta S = 0$ can be violated if the LS coupling is broken. In such a situation the intercombination transitions through triplet intermediate states is possible. We have observed the ion signal for two-photon resonances from the Ca ground state to $4p^2\ {}^3\mathrm{P}_2$ state. This state is a triplet state while the ground state and $4s4p\ {}^1\mathrm{P}_1$ states

are the singlet ones. The intensity of the observed resonance leaves no more doubts that this resonance occurs through the triplet state.

3.2 Order of the Ca states

The theoretical analysis of Ca photoionization in the examined range of wavenumbers has revealed the positions of the essential states excited by two-photons: $4s6s\ ^1S_0$, $4p^2\ ^1D_2$ and $4p^2\ ^1S_0$. The papers published before 1985 were based mainly on the data from Moore [24] where the order of states had been: $4p^2\ ^1S_0$ – 40 690 cm^{-1}, $4p^2\ ^1D_2$ – 40 720 cm^{-1}, $4s6s\ ^1S_0$ – 41 786 cm^{-1}. On the other hand the papers published after 1985 have used the data from paper of Sugar et al. [25] where the order of $4s6s\ ^1S_0$ (40 690 cm^{-1}) and $4p^2\ ^1S_0$ (41 786 cm^{-1}) states had been changed for the same wavenumbers as in the paper [24]. This correction introduced in the paper [25] has been explained by the quantum defect calculations done by Risberg [27]. In this paper Risberg explained that this change of the relative positions of Ca states gave a better fitting of the $4s6s\ ^1S_0$ state to all the series of $4s\ ms\ ^1S_0$ states and attributing the $4p^2\ ^1S_0$ state to the level 41 786 cm^{-1} should give a better ordering according to the theoretical ordering of three states of $4p^2$ configuration: ^{3}P, ^{1}D, ^{1}S.

Note that while the ordering of Sugar et al. [25] and Risberg [27] is in agreement with the general Hund's rules, the ordering of Moore [24] better agrees with a regular behaviour of the whole series of $4s\ ms\ ^1S_0$ states. In our opinion the explanation given by Risberg [27] is not satisfactory because the author has not given any calculations nor references.

Our results obtained during the three-photon ionization due to the autoionizing states can support the proposed change of order of the $4s6s\ ^1S_0$ and $4p^2\ ^1S_0$ states as given in paper of Sugar et al. [25]. As it was mentioned before (see Figs. 3 and 4) it seems that the two-photon resonant transition probability to the autoionizing states should be larger in the case of the intermediate state $4p^2$ than in the case of $4s6s$ configuration. Moreover, autoionizing states are highly excited states with two electron excitations, so an intermediate resonance with two electrons excitation should stimulate this process. We will show later that during the three-photon ionization due to autoionizing states the enhancement of the ion signal observed for the wavenumbers about 41 786 cm^{-1} is correlated with the two-photon $4p^2\ ^1S_0$ resonance.

3.3 Experimental two-photon resonant excitation and lifetime measurement

The two-photon resonant excitation to the bound $4p^2\ ^1S_0$ Ca states have been performed for the lower laser intensities. In such a case the population of the excited bound state of Ca was a function of the probability of a radiative decay and low probability of the ionization by the third photon. The measurement of the decay of $4p^2\ ^1S_0$ Ca state consisted in the measuring of

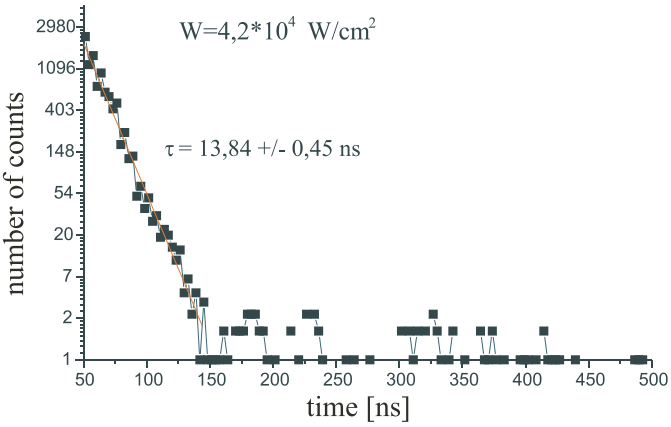

Fig. 5. The example of one radiative decay of $4p^2\ ^1S_0$ Ca state with two-photon resonant excitation.

478 nm fluorescence due to the transition from $4p^2\ ^1S_0$ to $4s4p\ ^1P_1$ and was performed for the laser intensity of order of 10^4 W/cm^2. We have compared results obtained for 10^4 laser shots for several laser intensities. An example of our results is shown in Figure 5. Taking into account that the laser pulse duration is 10 ns, the results presented in Figure 5 are obtained without the time deconvolution procedure. We assume that the plot of photon counts vs. time scale, 50 ns after the laser shot depends only on the decay of the atomic bound state. Because the results do not depend on the laser intensity in the range of the intensities variation we can assume that the measuring of $4p^2\ ^1S_0$ Ca state decay is stimulated only by the radiative decay while the third photon ionization process can be neglected. The averaged lifetime obtained by us is $\tau = 13.91 \pm 0.45$ ns and is close to those measured by Havey et al. [28] (12.6 ns) and Smith [29] (13.3 ns) as well as calculated by Mitroy [30] (12.5 ns).

4 Three-photon resonances above the ionization limit

In the simplest case three-photon resonances due to the autoionizing states are described in terms of a single electron excitation and/or ionization. This means that exactly one of the spinorbitals in the initial (usually ground) atomic state is replaced by a spinorbital representing an excited or liberated electron. However, some of the experimental results concerning, e.g., cross-sections for photoionization [31–35] or angular distributions of photoelectrons [36–39] cannot be adequately interpreted in terms of one-electron processes. One must thus take into account the channels including a double ionization, an ionization of one electron accompanied by an excitation of another one or an excitation of two electrons. In the latter two cases the excited states may be autoionizing states, the decay of which leads to the ionization. The problem whether the transitions of the two electrons occur simultaneously or rather have a character of a two-step process is a key problem in the investigations of the ionization dynamics.

4.1 The analysis of the highly excited Ca states

The exploration of a range of the laser photon wavenumber ν_L between 18 600 cm^{-1} and 20 930 cm^{-1} gives the possibility of finding many three-photons transitions due to the autoionizing states [14]. In the experiment the three-photon energy transfer ($\nu = 3\nu_L$) in the vicinity of the two-photon resonance of the $4s6s\ ^1\mathrm{S}_0$, $4p^2\ ^1\mathrm{S}_0$, $4p^2\ ^1\mathrm{D}_2$, $4s4d\ ^1\mathrm{D}_2$ and $4p^2\ ^3\mathrm{P}_\mathrm{J}$ bound states of Ca has been performed. Taking into account that the Ca ionization limit is 49 306 cm^{-1} [24,25] we can expect among such three-photon processes either photoionization or an excitation to highly excited Ca states.

In Section 3, we have mentioned the light polarization effects which are connected with the order of transitions and the selection rules. We also have to take into account that between the $4s$ threshold (limit of the first ionization) and the $3d$ threshold, doubly excited states are reached by an absorption of three photons and must be of odd parity, as in a single photon absorption [6,25]. Note that the $4s^2\ ^1\mathrm{S}_0$ ground state includes the $4s^2$, $4p^2$ and $3d^2$ configurations [40] which implies that one can expect the $3d\ mp$, $3d\ mf$, $3d\ mh$ and $4p\ 5s$ configurations leading to resonances in the examined wavenumber range. Any observed resonance in a single-photon absorption must have $J = 1$ but in three-photon absorption, $J = 3$ is also allowed. Moreover, we can expect that for two-photon resonance near the $4p^2\ ^1\mathrm{D}_2$ bound state the third photon can reach an autoionizing state with $J = 3$. If our laser beam is circularly polarized we will observe the resonances allowed for the three-photon absorption with $\Delta M = \Delta J = 3$ [14].

We will also study three-photon resonant processes with the third photon hitting a highly excited state located above the continuum edge. Such states are strongly coupled with the continuum, which opens a new ionization channel [41]. The well-known problem of classification of highly excited states, where the change of two valence electrons spinorbitals takes place, has been considered many years ago in papers devoted to the quantum defect [42–45] and the notation introduced in those papers is still used. If two electron spinorbitals in such a way that in the type $nl\ ml'$, $n \cong m$, they are known as "Wannier's states", and if $n \ll m$ they are known as "planetary states" [46]. Such highly excited states are in most cases autoionizing states, i.e. states for which the probability of a decay (coupling with the continuum) is large then the probability of an electron recombination to lower energy states.

A was shown earlier [14,40] the ground state of all atoms of alkaline earths, does not belong only to the configurations ns^2 but also to the configurations np^2 and $(n-1)d^2$. In such a situation the amplitudes of bound-continuum transitions: $ns^2 - ns\ mp$ or $ns\ mf$, $np^2 - np\ ms$ or $np\ md$; could be found simultaneously. This means that even in the simplest case of one-photon transitions (VUV) and ionization, an interpretation of the obtained spectra is not straight forward because of initial state being a mixture of configurations. For multiphoton processes in atoms with two valence electrons three-photon transition probabilities to highly excited states are enhanced if the excitation occurs in a one- or two-photon resonant way. The intermediate bound states are the states belonging to the configurations for which both electrons change the spinorbitals, for instance np^2 and nd^2. Such states are more strongly coupled with the autoionizing states $3d\ mp$, $3d\ mf$ than those with one of the electrons being $4s$.

4.2 The analysis of the Fano profile

We should realize at this moment that the sequence of excitations leading to one autoionizing state due to multiphoton absorption can play a significant role in the shape of the observed resonances. The shape of autoionizing profile is described by Fano profile [24] $I(\tilde{\nu})$:

$$I(\tilde{\nu}) = \sigma_a \frac{(\varepsilon(\tilde{\nu}) + q)^2}{1 + \varepsilon(\tilde{\nu})^2} \tag{1}$$

where: σ_a is a normalizing factor, $\varepsilon(\tilde{\nu}) = 2(\tilde{\nu}_L - \tilde{\nu}_R)/\Gamma$ is normalized wavenumber difference between excitation (laser) wavenumber $\tilde{\nu}_L$ and resonance wavenumber $\tilde{\nu}_R$ expressed in units of the profile halfwidth $\Gamma/2$, and q is the asymmetry parameter. The main role in the shape of autoionizing profiles is played by the parameter q. This parameter gives the ratio of two possible transition amplitudes: the transition through a highly excited decaying state or the transition directly to the continuum. The shape of the Fano profile is symmetric when $q \to \infty$. This means that the channel due to the autoionizing state is dominant compared to the second channel due to the direct transition to the continuum. If the coupling between the intermediate bound state and the autoionizing state is strong enough (the resonance coupling) the Fano profile should be symmetric. In this case the parameter q of the profile asymmetry should take a large value and the autoionization channel should be dominant. On the other hand if the coupling between the bound intermediate state and the higher (autoionizing) state is not very large the contribution of the autoionizing channel in ionization process decreases. If the bound–high autoionizing state transition is farther from the resonance the contribution of the autoionizing channel decreases while the direct ionization channel starts to be dominant. This makes important an experimental examination of the autoionization spectrum profiles and the order of excitation in such processes.

The second important parameter concerning the shape of the autoionizing resonance is the absorbed energy. For the two-electron "Wannier's states" only symmetric Fano profiles are observed. This is caused by the energy (wavenumbers) of those states being not so far from the second ionization limit and as a consequence by very short picosecond decay times of those states. In such a situation the coupling between those states and the bound intermediate states has to be strong so in this case the symmetric peak should be observed.

In experimental investigations of photoionization asymmetric Fano profiles due to autoionizing states are observed mainly near the first ionization limit. In this spectral region a good separation of the peaks due to the

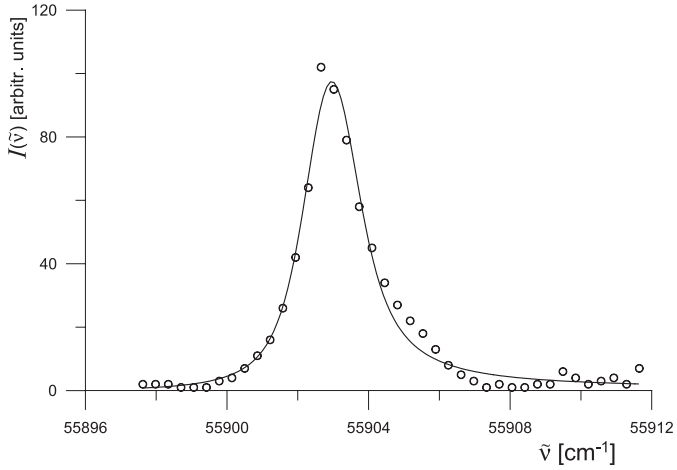

Fig. 6. Ionization yield for three-photon resonance to the $3d4f\ ^3\mathrm{D}_1$ autoionizing state in $\nu = 3\nu_L$ scale. The asymmetry Fano parameter $q = 19.6$. Points denote experimental data, solid line – fitted profile.

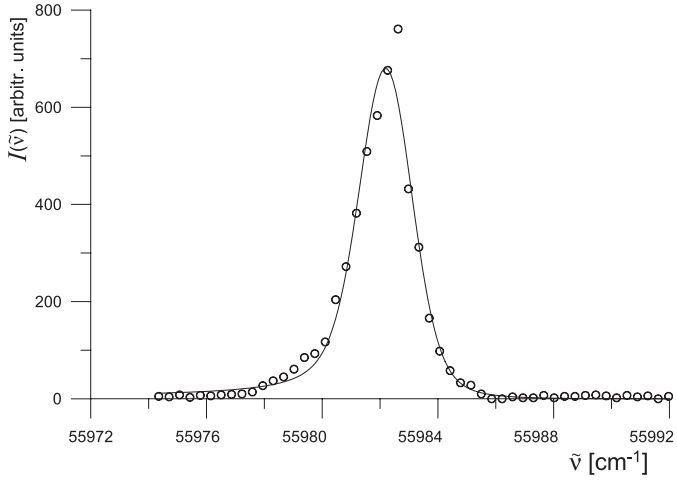

Fig. 7. Ionization yield for three-photon resonance to the $3d4f\ ^1\mathrm{P}_1$ autoionizing state in $\nu = 3\nu_L$ scale. The asymmetry Fano parameter $q = -24.1$. Points denote experimental data, solid line – fitted profile.

autoionizing state makes it possible to observe the asymmetric Fano profiles. For the peaks of the autoionization series located farther from the first ionization limit the density of the peaks increases and many Fano profiles can overlap. An overlap of many asymmetric Fano profiles can give as a consequence a symmetric profile.

In Figures 6 and 7 the ionization signal due to a three-photon resonance to the autoionizing states belonging to the configuration $3d4f$ and indicated as $^3\mathrm{D}_1$ and $^1\mathrm{P}_1$ in LS coupling scheme is shown. The three-photon resonance is obtained in the two-photon resonance close to the $4s4d\ ^1\mathrm{D}_2$ bound state. The profiles are asymmetric and the registered line shape $O(\tilde{\nu})$ is a convolution of the

Table 1. The best-fit values of the Fano line shape parameters: line halfwidth Γ, asymmetry parameter q. The halfwidth of excitation function fixed as equal to $\gamma_G = 1.5$ cm $^{-1}$.

State	Γ [cm^{-1}]	q
	$J = 1$	
$3d4f\ ^3\mathrm{D}_1$	1.09 (0.09)	19.6 (4.9)
$3d4f\ ^1\mathrm{P}_1$	0.96 (0.07)	–24.1 (0.1)
$3d15f\ ^1\mathrm{P}_1$	1.4 (7.1)	–15 (160)
$3d16f\ ^3\mathrm{D}_1$	6.6 (2.7)	–12 (21)
$3d16f\ ^1\mathrm{P}_1$	10.8 (4.3)	–17 (74)
$3d17f\ ^3\mathrm{P}_1$	6.6 (2.3)	18 (90)
	$J = 3$	
$3d8f$ I	5.54 (0.49)	–8.2 (1.2)
$3d8f$ II	5.64 (0.52)	–12.1 (3.3)
$3d8f$ III	5.66 (0.54)	–21 (13)
$3d8f$ IV	8.25 (0.50)	–8.5 (1.5)
$3d9f$ I	7.89 (0.97)	–30 (40)
$3d9f$ II	6.42 (0.69)	–29 (37)
$3d9f$ III	8.5 (1.3)	5.6 (2.2)
$3d9f$ IV	11.06 (0.91)	–9.0 (2.2)

Fano profile $I(\tilde{\nu})$ and the excitation function $I_E(\tilde{\nu})$:

$$O(\tilde{\nu}) = I(\tilde{\nu}) \otimes I_E(\tilde{\nu}) = \int_{-\infty}^{\infty} I(\tilde{\nu} - \tilde{\nu}') I_E(\tilde{\nu}') d\tilde{\nu}'. \qquad (2)$$

The excitation function $I_E(\tilde{\nu})$ is assumed in the form of the Gaussian profile:

$$I_E(\tilde{\nu}) = \frac{2\sqrt{\ln 2}}{\gamma_G \sqrt{\pi}} \exp\left[-\frac{4 \ln 2}{\gamma_G^2} \tilde{\nu}^2\right] \qquad (3)$$

where γ_G is its half-width.

In the line shape analysis we fitted $O(\tilde{\nu})$ profiles to our experimental data. The best fit procedure was performed using the Levenberg-Marquardt algorithm [47]. Our numerical fit allowed four parameters to vary: normalizing factor σ_a, resonance wavenumber $\tilde{\nu}_R$, line halfwidth Γ, the asymmetry parameter q while the halfwidth of the excitation function (many procedures based on the least-squares algorithm had been performed in order to establish γ_G parameter) has been fixed as equal to $\gamma_G = 1.5$ cm^{-1}. In the fitting procedure we took extreme care to verify if we reached the global minimum of chi-square sum as its local minimum may lead to significant errors in data analysis. The normalizing factor σ_a, resonance wavenumber $\tilde{\nu}_R$ do not play any essential role in our investigation and will not be discussed here. The other best-fit parameters determined for investigated lines are listed in Table 1.

On the far wing of the two-photon resonant transition $4s^2\ ^1\mathrm{S}_0$–$4p^2\ ^1\mathrm{D}_2$ there are three-photon resonances due to autoionizing states with $J = 3$. Taking into account that $3d\ mf$ $(J = 3)$ series has four components for each m [11,14] we have identified the resonance to the $3d8f$ autoionizing state and the fourth components are

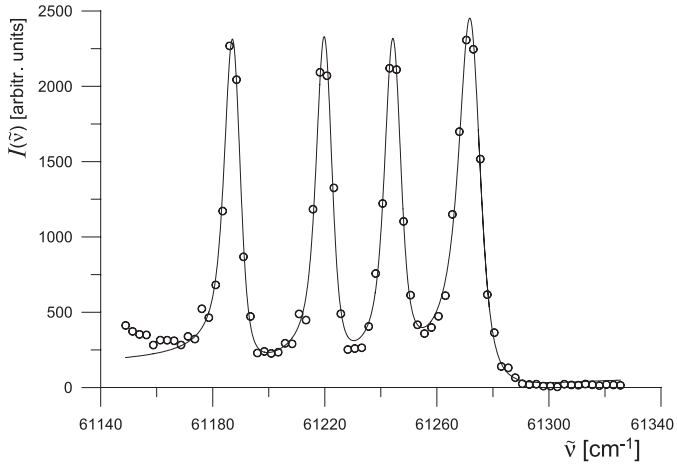

Fig. 8. Ionization yield for three-photon resonance to the $3d8f$ ($J = 3$) autoionizing state in $\nu = 3\nu_L$ scale. The asymmetry Fano parameters $q = -8.2$; –12.1; –20.9; –8.5. Points denote experimental data, solid line – fitted profile.

shown in Figure 8. In this case also the Fano profile can be fitted to experimental data.

The profiles for other autoionizing states studied in this experiment are symmetric in thus part of this spectrum from 60 900 cm^{-1} to 62 800 cm^{-1} for three photon laser excitation.

5 Conclusions

The results obtained in this paper during the three-photon ionization experiment suggest that the relative position of $4s6s$ $^1S_0$ and $4p^2$ $^1S_0$ states predicted by Sugar [25] is correct. Moreover in this experiment the two-photon resonant excitation to the $4p^2$ $^1S_0$ have been performed and the measurement of the decay of this state have been also determined.

We also discussed two possible ways of the two electron excitation which is connected to the problem of a classification of highly excited states. One must thus take into account the channels including a double ionization, an ionization of one electron accompanied by an excitation of another one or an excitation of two electrons. In the latter two cases the excited states may be autoionizing states, which decay leading to the ionization.

From the analysis of the Fano profiles we have obtained the corresponding values of asymmetry parameters q (see Tab. 1), line halfwidth Γ, and consequently time decay $\tau = 1/c\Gamma$ (where c – speed of light) of the high lying Ca states (see Tab. 2).

The analysis of the Fano profile have been performed only for well separated three-photon transitions above the ionization limit (see Tab. 1) for $J = 1$ and $J = 3$. If the coupling between the bound intermediate state and the higher (autoionizing) state is not very large the contribution of the autoionizing channel in such a process decreases. Since the bound–high autoionizing state transition is farther from the resonance the contribution of the autoionizing channel decreases, and therefore the direct three-photon ionization channel becomes dominant, so that the Fano asymmetry parameter q decreases. In our case the Fano parameter is of the order of 10–30, so we can say that both channels play a role in that transitions, but the direct ionization channel can be dominant. Such measurements yield important experimental information on the autoionization spectrum profiles and the sequence of excitation in such processes.

Table 2. The time decays τ (in 10^{-12} s) of some autoionizing states.

State	τ[ps]
$J = 1$	
$3d4f$ $^3D_1$	30.58 (2.6)
$3d4f$ $^1P_1$	34.7 (2.6)
$3d15f$ $^1P_1$	24 (121)
$3d16f$ $^3D_1$	5.05 (2.1)
$3d16f$ $^1P_1$	3.09 (1.3)
$3d17f$ $^3P_1$	5.05 (1.8)
$J = 3$	
$3d8f$ I	6.02 (0.54)
$3d8f$ II	5.9 (0.55)
$3d8f$ III	5.9 (0.57)
$3d8f$ IV	4.04 (0.25)
$3d9f$ I	4.2 (0.52)
$3d9f$ II	5.2 (0.56)
$3d9f$ III	3.9 (0.61)
$3d9f$ IV	3.01 (0.25)

As is well-known the lifetime of the low-lying bound states are of the order of hundred of ns. The result of the present paper as well as other experimental [28,29] and theoretical [30] results give the values of ten's ns for the lifetime of the bound high-lying Ca states. For excitation of the Rydberg states, for instance of Li_2 [4] the effective lifetimes of the Rydberg levels has been also determined from the linewidth parameter Γ from the Fano model. According to reference [4] the lifetimes decrease from 350 to 230 ps with the increase of the transitions energy, which demonstrates the strong coupling of an final levels with the ionization continuum, compared to the radiation decay channel. As we mentioned before the measured lifetime of these states with high principal quantum number n are often larger by several orders of magnitude than was expected from the general rule $\tau_n \approx n^3$. The reason of these discrepancies is due to the line profiles of optical transitions to these Rydberg states which depend not only on the radiative lifetimes of these states but also on several nonradiative decay channels such as autoionization or even predissociation, which may shorten the lifetimes determined from the Γ parameter.

In Table 2 the values of the time decays τ of the autoionization states are listed. Those states which belong just to the ionization limit have the decay time of 30 ps while the decay time of the higher states compare to the ionization limit (in energy scale) are of 6–3 ps. Such highly

excited states are in most cases autoionizing states, the probability of decay is larger and than the probability of an electron recombination to lower energy states. On the other hand, in such a case the determination of the decay of the highly excited states can inform about recognizing that there are transitions to the autoionizing states or bound-continuum transitions. We can simple conclude that the higher state are stronger coupled with the continuum and the second channel (direct ionization) could be dominant.

The errors which are indicated in Table 1 for both Fano parameters Γ and q are due to the overlapping profiles belonging to other autoionizing states observed in this experiment.

The authors wish to thank to the referees for pointing out several errors in the original manuscript.

References

1. F. Merkt, R.N. Zare, J. Chem. Phys. **101**, 3495 (1994)
2. W.G. Scherzer, H.L. Selzle, E.W. Schlag, R.D. Levine, Phys. Rev. Lett. **72**, 1435 (1994)
3. L.A. Pinnaduwage, Y. Zhu, Chem. Phys. Lett. **277**, 147 (1997)
4. M.A. Baig, F. Bylicki, M. Keil, J. Zhu, W. Demtroder, ICSLS **11**, 275 (2001)
5. D.T. Alimov, A.N. Bielkowskij, A.I. Gajsak, O.I. Zacarinnyj, W.I. Lendiel, W. Miediediewa, D.M. Pietrina, I.M. Szuba, Ukr. Fiz. Zurn. **33**, 658 (1988)
6. S.M. Farooqi, J.P. Connerade, C.H. Green, J. Marangos, M.H.R. Hutchinson, N. Shen, J. Phys. B: At. Mol. Phys. **24**, L179 (1991)
7. S. Assimopoulos, A. Bolovinos, A. Jimoyiannis, P. Tsekeris, E. Luc-Koenig, M. Aymar, J. Phys. B: At. Mol. Opt. Phys. **27**, 2471 (1994)
8. E. Luc–Koenig, A. Bolovinos, M. Aymar, S. Assimopoulos, A. Jimoyiannis, P. Tsekeris, Z. Phys. D **32**, 49 (1994)
9. A. Bolovinos, E. Luc–Koenig, S. Assimopoulos, A. Lyras, N.E. Karapanagioti, D. Charalambidis, M. Aymar, Z. Phys. D **38**, 265 (1996)
10. M. Strehle, U. Weichmann, G. Gerber, Phys. Rev. A **58**, 450 (1998)
11. J.O. Gaardsted, T. Andersen, H.K. Haugen, J.E. Hansen, N. Veack, J. Phys. B: At. Mol. Phys. **24**, 4363 (1991)
12. R.S. Dygdała, A. Zawadzka, M. Zieliński, *Int. Conf. LASER'97, Proc. Soc. Optical and Quantum-Electronics*, New Orleans, December 15-19, 1997, p. 311
13. R.S. Dygdała, K. Karasek, F. Giammanco, J. Kobus, A. Pabjanek-Zawadzka, A. Raczynski, J. Zaremba, M. Zieliński, J. Phys. B: At. Mol. Opt. Phys. **31**, 2259 (1998)
14. A. Zawadzka, R.S. Dygdała, A. Raczyński, J. Zaremba, J. Kobus, J. Phys. B: At. Mol. Phys. **35**, 1801 (2002)
15. F. Giammanco, Phys. Rev. A **40**, 5160 (1989)
16. F. Giammanco, Phys. Rev. A **40**, 5171 (1989)
17. F. Giammanco, Phys. Rev. A **43**, 6939 (1991)
18. F. Giammanco, N. Spinelli, *Plasma collective effects in atomic physics*, edited by F. Giammanco, N. Spinelli (EDS, Edizioni Tecnico-Scientifische, Pisa, Italy, 1996)
19. R.S. Dygdała, K. Karasek, K. Stefański, A. Zawadzka, R. Rumianowski, M. Zieliński, J. Phys. D: Appl. Phys. **33**, 41 (2000)
20. U. Fano, Phys. Rev. **124**, 1866 (1961)
21. N.F. Ramsay, *Molecular beams* (Clarendon Press, Oxford, 1956)
22. M. Zieliński, K. Karasek, R.S. Dygdała, Rev. Sci. Instr. **67**, 3325 (1996)
23. R.S. Dygdała, F. Fuso, E. Arimondo, M. Zieliński, Rev. Sci. Instr. **66**, 3507 (1995)
24. C.E. Moore, *A multiplet table of astrophysical interest* (Natl. Bur. Stand. Tech., Washington, 1959)
25. J. Sugar, G. Corliss, J. Phys. Chem. Ref. Data, Suppl. **2**, 51 (1985)
26. V.P. Shevelko, *Atoms and their spectroscopic properties*, Springer Series on Atoms and Plasma (Springer, 1997)
27. G. Risberg, Ark. Fys. **37**, 231 (1969)
28. M.D. Havey, I.C. Balling, J.J. Wright, J. Opt. Soc. Am. B **67**, 488 (1977)
29. G. Smith, J. Phys. B: At. Mol. Opt. Phys. **21**, 2827 (1988)
30. J. Mitroy, J. Phys. B: At. Mol. Phys. **26**, 3703 (1993)
31. N. Karamatsos, M. Mueller, M. Schmidt, P. Zimmermann, J. Phys. B: At. Mol. Phys. **18**, L107 (1985)
32. U. Griesmann, N. Shen, J.P. Connerade, K. Sommer, J. Hormes, J. Phys. B: At. Mol. Phys. **21**, L83 (1988)
33. M.C. Noecker, B.P. Masterson, C.E. Wieman, Phys. Rev. Lett. **61**, 310 (1988)
34. S.A. Blundell, W.R. Johnson, J. Sapirstein, Phys. Rev. Lett. **65**, 1411 (1990)
35. V.K. Ivanov, J.B. West, J. Phys. B: At. Mol. Phys. **26**, 2099 (1993)
36. D. Feldmann, K.H. Welge, J. Phys. B: At. Mol. Phys. **15**, 1651 (1982)
37. C. Kerling, N. Bowering, U. Heinzmann, J. Phys. B: At. Mol. Phys. **23**, L629 (1990)
38. S. Baier, A.N. Grum-Grzhimailo, N.M. Kabachnik, J. Phys. B: At. Mol. Phys. **27**, 3363 (1994)
39. H. Lagadec, B. Carre, D. Porterat, P.R. Fourier, M. Aymar, J. Phys. B: At. Mol. Phys. **29**, 471 (1996)
40. N. Vaeck, M. Godefroid, I.E. Hansen, J. Phys. B: At. Mol. Phys. **24**, 361 (1991)
41. T. Ishihara, K. Hino, J.H. McGuire, Phys. Rev. A **44**, (1991)
42. M.S. Seaton, Rep. Prog. Phys. **46**, 167 (1983)
43. P. Camus, M. Dieulin, A. El Himdy, Phys. Rev. A **26**, 379 (1982)
44. R.M. Jopson, R.R. Freeman, W.E. Cooke, J. Bokor, Phys. Rev. Lett. **51**, 1640 (1983)
45. R.M. Jopson, R.R. Freeman, W.E. Cooke, J. Bokor, Phys. Rev. A **29**, 3154 (1984)
46. L.F. DiMauro, D. Kim, M.W. Courtney, M. Anselment Phys. Rev. A **38**, 2338 (1988)
47. W.H. Press, S.A. Teukolsky, W.T. Vetterling, B.P. Flannery *Numerical Recipes in Fortran. The Art of Scientific Computing,* 2nd edn. (Cambridge University Press, 1992), p. 678